

Combining checkpointing and data compression for large scale seismic inversion

Navjot Kukreja
Imperial College London
London, UK
n.kukreja@imperial.ac.uk

Jan Hückelheim
Imperial College London
London, UK

Mathias Louboutin
Georgia Institute of Technology
Atlanta, GA, USA

Kaiyuan Hou
Northwestern University
Evanston, IL, USA

Fabio Luporini
Imperial College London
London, UK

Paul Hovland
Argonne National Laboratory
Lemont, IL, USA

Gerard Gorman
Imperial College London
London, UK

Abstract—Seismic inversion and imaging are adjoint-based optimization problems that processes up to terabytes of data, regularly exceeding the memory capacity of available computers. Data compression is an effective strategy to reduce this memory requirement by a certain factor, particularly if some loss in accuracy is acceptable. A popular alternative is checkpointing, where data is stored at selected points in time, and values at other times are recomputed as needed from the last stored state. This allows arbitrarily large adjoint computations with limited memory, at the cost of additional recomputations.

In this paper we combine compression and checkpointing for the first time to compute a realistic seismic inversion. The combination of checkpointing and compression allows larger adjoint computations compared to using only compression, and reduces the recomputation overhead significantly compared to using only checkpointing.

Index Terms—Checkpointing, compression, adjoints, inversion

I. INTRODUCTION

Adjoint-based optimization problems typically consist of a simulation that is run forward in simulation time, producing data that is used in reverse order by a subsequent adjoint computation that is run backwards in simulation time. Figure 2 shows the resulting data flow. Many important applications in science and engineering have this structure, including seismic inversion.

In seismic inversion, the propagation of seismic waves through the earth's subsurface is simulated and compared with data from field measurements. The model of the subsurface is iteratively improved by minimizing the misfit between simulated data and field measurement in an adjoint optimization problem. Figure 1 shows the setup of the field experiment that produces the measured data [18]. Storing all intermediate results as required for the data flow shown in Figure 2 is not feasible, since this would require tens of terabytes of memory, which is not commonly available on the machines used to solve these problems. To solve this problem, a number of strategies are used that are discussed in the following paragraphs. While this paper uses seismic inversion as a test case, most of these ideas, including the one presented in

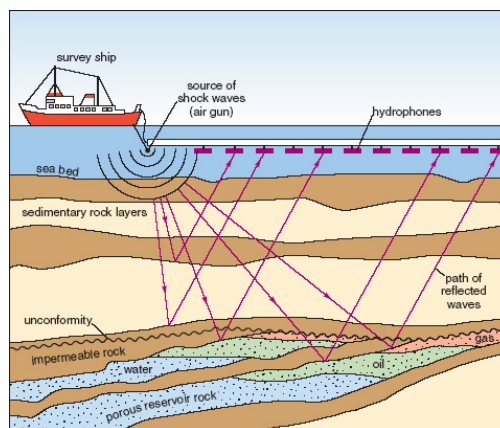


Fig. 1. Illustration of an offshore seismic survey that collects the input data for seismic inversion. Source: The Open University [2]

this work, are also applicable to other adjoint optimization problems.

Domain decomposition is often used not only to distribute the computational workload across more processors, but also to utilize the large amount of memory available in distributed systems. While this strategy is very powerful, the number of compute nodes and therefore the amount of memory that can be used efficiently is limited, for example by communication overheads that start to dominate as the domain is split into increasingly small pieces [22]. Secondly, this method is broadly used on conventional clusters but can be drastically more complicated to setup and slower due to the communication in a cloud-based setup. Another common strategy in seismic inversion is to only store values at the boundaries of the domain at each timestep, and reconstruct the rest of the wavefield when required [6], [24] with time reversal of the wave equation. However, this method is not applicable for wave equations that are not time reversible when for example physical attenuation is included.

Checkpointing is yet another strategy to reduce the memory overhead. Only a subset of the program states during the

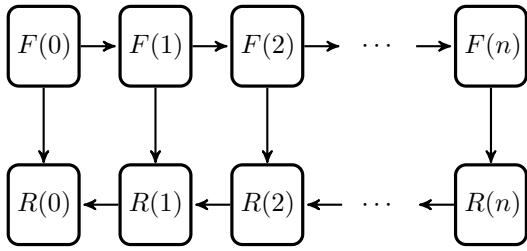


Fig. 2. The dataflow pattern that is typical of adjoint-based optimization problems

forward pass is stored (and the rest discarded). The discarded data is recomputed when needed by restarting the forward pass from the last available stored state. The Revolve algorithm [11] provides an answer to the question of which states should be stored and which states should be recomputed to minimize the total amount of recomputation work. Other authors have subsequently developed extensions to Revolve that are optimal under different assumptions [4], [19], [21], [23].

Data compression is also increasingly used to reduce the memory footprint of scientific applications. General purpose data compression algorithms like Zlib (which is a part of gzip) [9], and compression algorithms for video and image data such as JPEG-2000 [20] have been presented in previous work. More recently, special purpose compression algorithms for floating-point scientific data have been developed, such as ZFP or SZ [10], [12], [14].

Lossless algorithms guarantee that the exact original data can be recovered during decompression, whereas lossy algorithms introduce an error, but often guarantee that the error does not exceed certain absolute or relative error metrics. Typically, lossy compression is more effective in reducing the data size. Most popular compression packages offer various settings that allow a tradeoff between compression ratio, accuracy, and compression and decompression time.

It is worth noting that another data reduction strategy is to typecast values into a lower precision format, for example, from double precision to single precision. This can be seen as a computationally cheap lossy compression algorithm with a compression ratio of 2.

Perhaps counterintuitively, compression can not only reduce the memory footprint, but also speed up an application. Previous work has observed that the compression and decompression time can be less than the time saved from the reduction in data that needs to be communicated across MPI nodes or between a GPU and a host computer [17].

Another way of using compression to speed up adjoint-based methods is to use it *instead* of checkpointing. If the compression ratio is sufficient to fit the entire data in memory, checkpointing is no longer necessary. Previous work has discussed this in the context of computational fluid dynamics [7] and seismic inversion using compression algorithms specifically designed for wavefields [5], [8].

In this paper, we extend the previous studies by *combining*

checkpointing and compression. This is obviously useful when the data does not fit in the available memory even after compression, for example for very large adjoint problems, or for problems where the required accuracy limits the achievable compression ratios.

Compared to the use of only checkpointing without compression, our combined method often improves performance. This is a consequence of the reduced size of stored program states, allowing more program states to be stored during the forward computation. This in turn reduces the amount of recomputation that needs to be performed. On the other hand, the compression and decompression itself takes time. We therefore provide a comprehensive performance model that predicts whether the combined method is beneficial, that is, whether the time spent compressing and decompressing is less than the time saved by reduced recomputations.

For benchmarking we used a dual-socket Intel(R) Xeon(R) Platinum 8180M @ 2.50 Ghz (28 cores each), henceforth called Skylake. We discuss performance results for varying error tolerances for the lossy ZFP compression algorithm ranging from 10^0 to 10^{-15} , and different types of forward and adjoint computations that vary in their ratio between compute cost and state size.

Our aim is to make this discussion independent of the hardware, application and compression algorithm. We therefore do not discuss whether or not the accuracy of the decompressed data is sufficient for our application, or whether other algorithms might achieve a better accuracy/compression tradeoff.

II. TEST CASE USING DEVITO AND PYREVOLVE

We use Devito [15], [16] to solve forward and adjoint wave equation problems. Devito is a domain-specific language that enables the rapid development of finite-difference solvers from a high-level description of partial differential equations. The simplest version of the seismic wave equation is the acoustic isotropic wave equation defined as:

$$m(x) \frac{\partial^2 u(t, x)}{\partial t^2} - \Delta u(t, x) = q(t, x), \quad (1)$$

where $m(x) = \frac{1}{c^2(x)}$ is the squared slowness, $c(x)$ the spatially dependent speed of sound, $u(t, x)$ is the pressure wavefield, $\Delta u(t, x)$ denotes the laplacian of the wavefield and $q(t, x)$ is a source term. Some of our experiments in Section V are performed using a more accurate and more complex version of this equation called Tilted Transverse Isotropy (TTI) [25] that takes into account the anisotropic propagation of waves in the earth subsurface (directional dependency of the speed of sound). We leave the TTI equations out of this paper for brevity.

The solution to equation 1 forms the forward problem. The seismic inversion problem minimizes the misfit between simulated and observed signal given by:

$$\min_m \phi_s(m) = \frac{1}{2} \|d_{sim} - d_{obs}\|_2^2. \quad (2)$$

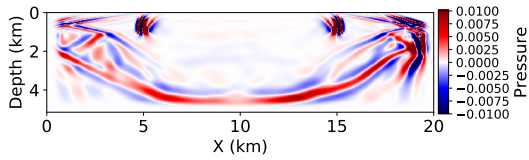


Fig. 3. Cross-section of the wavefield used as a reference sample for compression and decompression. This field was formed after a Ricker wavelet source was placed at the surface of the model and the wave propagated for 2500 timesteps. This is a vertical (x-z) cross-section of a 3D field, taken at the y source location

This optimization problem is usually solved using gradient based methods such as steepest descent, where the gradient is computed using the adjoint-state method that involves the data-flow pattern from Figure 2.

The values of $m(x)$ used in this work are derived from the Overthrust model [3] over a grid of $287 \times 881 \times 881$ points, including an absorbing layer of 40 points on each side. The grid spacing is 25m in space. The propagation time is 4sec that corresponds to 2500 timesteps. The wave field at the final time is shown in Figure 3, and only this field was used for the compression experiments in this paper. The uncompressed size of this single time step field is just under 900MB.

To implement Revolve with Devito, we use pyRevolve [13] which is a python wrapper for the Revolve algorithm. The performance model in section IV assumes that the implementation is similar to pyRevolve, which stores a checkpoint by copying a portion of the operator’s working memory to the checkpointing memory and similarly loads a checkpoint by copying from the checkpointing memory to the operator’s working memory. Although a perfect implementation of checkpointing may be able to avoid these copies, the overhead attached to these copies can be ignored for an operator that is sufficiently computationally intensive. However, we include the overheads in the model to verify this assumption.

III. COMPRESSION ALGORITHMS

A. Lossless

We use the python package *blosc* [1], which includes implementations for six different lossless compression algorithms, namely ZLIB, ZSTD, BLOSC LZ, LZ4, LZ4HC and Snappy. An exhaustive search over all available parameters resulted in a maximum compression ratio of 1.18x. We therefore focus on lossy compression in the remainder of this work.

B. Lossy

We use the lossy compression package ZFP [14] developed in C. To use ZFP from python, we developed a python wrapper for the reference implementation of ZFP.

ZFP supports three compression modes, namely fixed-tolerance, fixed-precision and fixed-rate. The fixed-tolerance mode limits the absolute error, while the fixed-precision mode limits the relative error to some user-specified value. The fixed-rate mode achieves a guaranteed compression ratio requested by the user, but does not provide any bounds on accuracy loss.

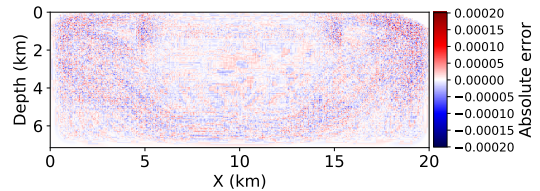


Fig. 4. Cross-section of the field that shows errors introduced during compression and decompression using the fixed-tolerance mode. It is interesting to note that the errors are more or less evenly distributed across the domain with only slight variations corresponding to the wave amplitude (from the field plot in Figure 3). A small block-like structure characteristic of ZFP can be seen.

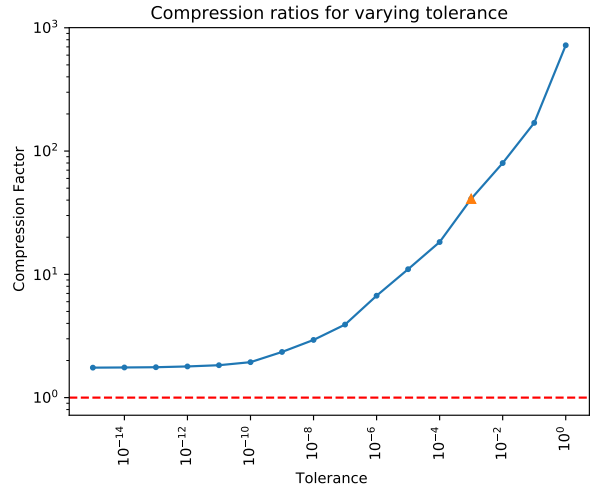


Fig. 5. Compression ratios achieved on compressing the wavefield. We define compression ratio as the ratio between the size of the uncompressed data and the compressed data. The dashed line represents no compression. The highlighted point corresponds to the setting used for the other results here unless otherwise specified.

Figure 5 shows compression ratios for a variety of settings for the three modes.

The compression ratio achieved per unit time spent during compressing and decompressing was seen to be highest in the fixed-tolerance mode albeit with highly unpredictable compression ratios. Figure 4 shows the spatial distribution of the error after compression and decompression, compared to the original field, using fixed-tolerance mode.

In our experiments using Devito, the time required to compress a checkpoint was in the same order of magnitude as the time taken to compute a timestep.

IV. PERFORMANCE MODEL FOR A COMBINATION OF REVOLVE AND COMPRESSION

We assume that the computation of a single forward time step takes the same wall time as the computation of a single reverse time step. We denote this time as C . For a simulation with N timesteps, the minimum wall time required for the full forward-adjoint evaluation is given by

$$T_N = 2 \cdot C \cdot N. \quad (3)$$

If the size of a single timestep in memory is given by \mathbf{S} , this requires a memory of at least size $\mathbf{S} \cdot \mathbf{N}$. If sufficient memory is available, no checkpointing or compression is needed.

If the memory is smaller than $\mathbf{S} \cdot \mathbf{N}$, Revolve provides a strategy to solve for the adjoint field by storing a subset of the \mathbf{N} total checkpoints and recomputing the remaining ones. The overhead introduced by this method can be broken down into the recomputation overhead \mathbf{O}_R and the storage overhead \mathbf{O}_S . The recomputation overhead is the amount of time spent in recomputation, given by

$$\mathbf{O}_R(N, M) = p(N, M) \cdot \mathbf{C}, \quad (4)$$

where $p(N, M)$ is the minimum number of recomputed steps from [11], reproduced here in equation 5. In equation 5, M is the number of checkpoints that can be stored in memory. Note that for $M \geq N$, \mathbf{O}_R would be zero. For $M < N$, \mathbf{O}_R grows rapidly as M is reduced relative to N .

In an ideal implementation, the storage overhead \mathbf{O}_S might be zero, since the computation could be done “in-place”, but in practice, checkpoints are generally stored in a separate section of memory and they need to be transferred to a “computational” section of the memory where the compute is performed, and then the results copied back to the checkpointing memory. This copying is a common feature of checkpointing implementations, and might pose a non-trivial overhead in some scenarios. This storage overhead is given by

$$\mathbf{O}_{SR}(N, M) = \mathbf{W}(N, M) \cdot \frac{\mathbf{S}}{\mathbf{B}} + \mathbf{R}(N, M) \cdot \frac{\mathbf{S}}{\mathbf{B}} \quad (6)$$

where \mathbf{W} is the total number of times Revolve writes checkpoints for a single run, \mathbf{R} is the number of times checkpoints are read, and \mathbf{B} is the memory bandwidth of the target system. The total time to solution becomes

$$T_R = 2 \cdot \mathbf{C} \cdot \mathbf{N} + \mathbf{O}_R(N, M) + \mathbf{O}_{SR}(N, M) \quad (7)$$

By using compression, the size of each checkpoint is reduced and therefore the number of checkpoints available is increased (M in equation 5). This reduces the recomputation overhead \mathbf{O}_R , while at the same time adding overheads related to compression and decompression in \mathbf{O}_S . To be beneficial, the reduction in \mathbf{O}_R must offset the increase in \mathbf{O}_{SR} , leading to an overall decrease in the time to solution T .

Our performance model assumes that the compression algorithm behaves uniformly across the different time steps of the simulation, i.e. that we get the same compression ratio, compression time and decompression time, no matter which of the N possible checkpoints we try to compress/decompress. The storage overhead now becomes

$$\mathbf{O}_{SR}(N, M) = \mathbf{W}(N, M \cdot F) \cdot \left(\frac{\mathbf{S}}{\mathbf{F} \cdot \mathbf{B}} + t_c \right) + \mathbf{R}(N, M \cdot F) \cdot \left(\frac{\mathbf{S}}{\mathbf{F} \cdot \mathbf{B}} + t_d \right) \quad (8)$$

where \mathbf{F} is the compression ratio (i.e. the ratio between the uncompressed and compressed checkpoint), and t_c and t_d are compression and decompression times, respectively. At the

same time, the recomputation overhead decreases because \mathbf{F} times more checkpoints are now available.

V. RESULTS

We can distinguish three different scenarios, depending on the amount of available memory.

- 1) If the memory is insufficient even with compression to store the entire trajectory, one can either use checkpointing only, or combine checkpointing with compression.
- 2) If the available memory is not sufficient to store the uncompressed trajectory, but large enough to store the entire compressed trajectory, we study the two possible strategies: Either use compression only, or use checkpointing only.
- 3) If the available system memory is large enough to hold the entire uncompressed trajectory, neither compression nor checkpointing is necessary.

All three scenarios can be seen in Figure 6. The second scenario was studied in previous work [7], while the combined method is also applicable to the first scenario, for which previous work has only used checkpointing without compression.

We can identify a number of factors that make compression more likely to be beneficial compared to pure checkpointing: A very small system memory size and a large number of time steps lead to a rapidly increasing recompute factor, and compression can substantially reduce this recompute factor. This can be seen in Figures 6 and 8.

The extent to which the recompute factor affects the overall runtime also depends on the cost to compute each individual time step. If the compute cost per time step is large compared to the compression and decompression cost, then compression is also likely to be beneficial, as shown in Figure 7. As the time per time step increases and the compression cost becomes negligible, we observe that the ratio between the runtime of the combined method and that of pure checkpointing is only determined by the difference in recompute factors.

VI. CONCLUSIONS AND FUTURE WORK

We use lossy compression to reduce the computational overhead of checkpointing in an adjoint computation used in full waveform inversion, a common method in seismic imaging applications whose memory footprint commonly exceeds the available memory size in high performance computing systems. We also developed a performance model that computes whether or not the combination of compression and checkpointing will outperform pure checkpointing or pure compression in a variety of scenarios, depending on the available memory size, computational intensity of the application, and compression ratio and throughput of the compression algorithm. Our current result has several limitations that we plan to address in future work:

- We do not discuss the accuracy of the results after decompression. This depends on the application, compression algorithm, and affects the achievable compression ratios. Our performance model only requires knowledge of the compression time and ratio, and it is up to the user of

$$p(N, M) = \begin{cases} N(N-1)/2, & \text{if } M = 1 \\ \min_{1 \leq \tilde{N} \leq N} \{ \tilde{N} + p(\tilde{N}, M) + p(N - \tilde{N}, M - 1) \}, & \text{if } M > 1 \end{cases} \quad (5)$$

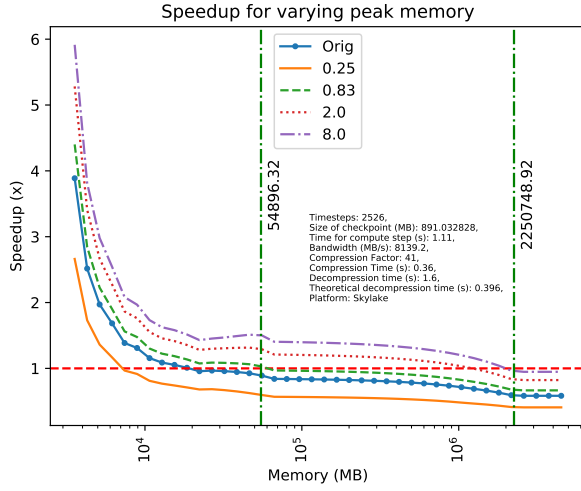


Fig. 6. The speedups predicted by the performance model for varying memory. The baseline (1.0) is the performance of a Revolve-only implementation under the same conditions. The different curves represent kernels with differing compute times (represented here as a factor of the sum of compression and decompression times). The first vertical line at 53GB marks the spot where the compressed wavefield can completely fit in memory and Revolve is unnecessary if using compression. The second vertical line at 2.2 TB marks the spot where the entire uncompressed wavefield can fit in memory and neither Revolve nor compression is necessary. The region to the right is where these optimisations are not necessary or relevant. The middle region has been the subject of past studies using compression in adjoint problems. The region to the left is the focus of this paper.

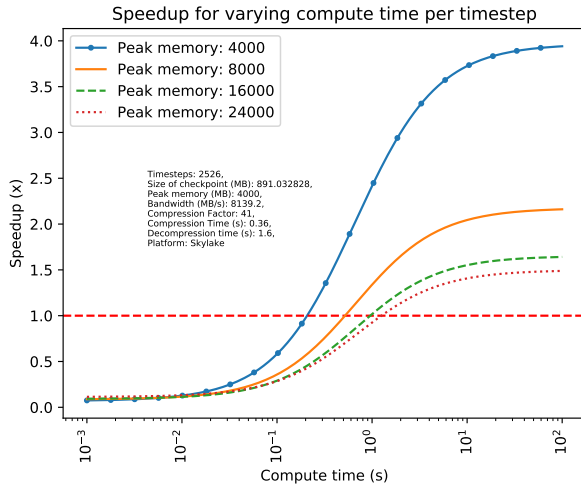


Fig. 7. The speedups predicted by the performance model for varying compute cost. The baseline (1.0) is the performance of a Revolve-only implementation under the same conditions. The benefits of compression drop rapidly if the computational cost of the kernel that generated the data is much lower than the cost of compressing the data. For increasing computational costs, the benefits are bounded.

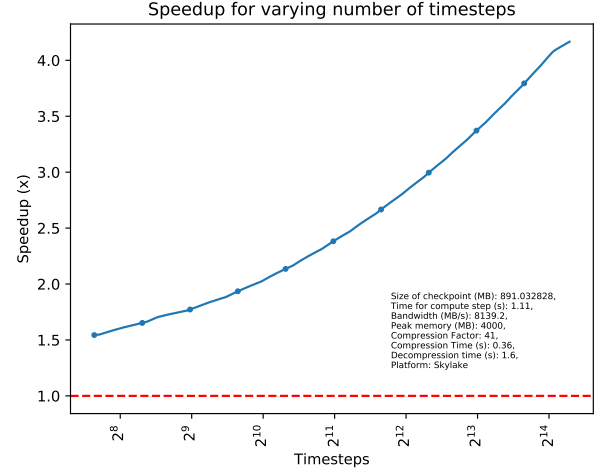


Fig. 8. The speedups predicted by the performance model for varying number of timesteps to be reversed. The baseline (1.0) is the performance of a Revolve-only implementation under the same conditions. It can be seen that compression becomes more beneficial as the number of timesteps is increased.

this model to determine what accuracy is needed and thus what compression ratio is realistic for their application.

- We only present results using the ZFP compression library. It would be interesting to try a greater variety of compression algorithms.
- ZFP only supports serial decompression. If ZFP supported parallel decompression, our experiments would likely show a greater region in which the combined method is faster than pure checkpointing. Furthermore, ZFP only supports fields with up to three dimensions, while exploiting similarities between fields at different time steps may yield a better compression ratio.
- Our performance model is based on uniform compression ratios and times. However, many applications, including FWI, are likely to have initial conditions that contain little information and are easily compressed, and the compression ratio gradually declines as the field becomes more complex. We based our experiments on the final wave field, which is presumably difficult to compress.
- In comparing pure compression with pure checkpointing, we assume that every checkpoint is compressed and decompressed. However, if the available memory is only slightly less than the required memory, an implementation that compresses only a subset of the checkpoints might outperform the expectations of our model.
- We do not discuss multi-level checkpointing, where some checkpoints are stored on a slower, larger device. We expect compression to be beneficial in these scenarios due to reduced data transfer sizes.

ACKNOWLEDGMENT

This work was funded by the Intel Parallel Computing Centre at Imperial College London and EPSRC EP/R029423/1. This work was supported by the U.S. Department of Energy, Office of Science, Office of Advanced Scientific Computing Research, Applied Mathematics and Computer Science programs under contract number DE-AC02-06CH11357. We would also like to acknowledge the support from the SINBAD II project and the member organizations of the SINBAD Consortium.

We gratefully acknowledge the computing resources provided and operated by the Joint Laboratory for System Evaluation (JLSE) at Argonne National Laboratory.

REFERENCES

- [1] Blosc (<http://blosc.org>).
- [2] Earth's physical resources: petroleum - detection, exploration and evaluation (continued) (<http://www.open.edu/openlearn/science-maths-technology/science/environmental-science/earths-physical-resources-petroleum/content-section-3.2.1>).
- [3] Fred Aminzadeh, N Burkhard, J Long, Tim Kunz, and P Duclos. Three dimensional SEG/EAGE models—an update. *The Leading Edge*, 15(2):131–134, 1996.
- [4] Guillaume Aupy, Julien Herrmann, Paul Hovland, and Yves Robert. Optimal multistage algorithm for adjoint computation. *SIAM Journal on Scientific Computing*, 38(3):C232–C255, 2016.
- [5] Christian Boehm, Mauricio Hanzich, Josep de la Puente, and Andreas Fichtner. Wavefield compression for adjoint methods in full-waveform inversion. *Geophysics*, 81(6):R385–R397, 2016.
- [6] Robert G Clapp. Reverse time migration with random boundaries. In *Seg technical program expanded abstracts 2009*, pages 2809–2813. Society of Exploration Geophysicists, 2009.
- [7] ERIC C Cyr, JN Shadid, and T Wildey. Towards efficient backward-in-time adjoint computations using data compression techniques. *Computer Methods in Applied Mechanics and Engineering*, 288:24–44, 2015.
- [8] F Rubio Dalmau, M Hanzich, J de la Puente, and N Gutiérrez. Lossy data compression with DCT transforms. In *EAGE Workshop on High Performance Computing for Upstream*, 2014.
- [9] Peter Deutsch and Jean-Loup Gailly. Zlib compressed data format specification version 3.3. Technical report, 1996.
- [10] Sheng Di, Dingwen Tao, Xin Liang, and Franck Cappello. Efficient lossy compression for scientific data based on pointwise relative error bound. *IEEE Transactions on Parallel and Distributed Systems*, 2018.
- [11] Andreas Griewank and Andrea Walther. Algorithm 799: Revolve: an implementation of checkpointing for the reverse or adjoint mode of computational differentiation. *ACM Transactions on Mathematical Software (TOMS)*, 26(1):19–45, 2000.
- [12] Christos Kaklamanis, Theodore Papatheodorou, PaulG. Spirakis, Jeremy Iverson, Chandrika Kamath, and George Karypis. *Lecture Notes in Computer Science*, volume 7484, chapter Fast and Effective Lossy Compression Algorithms for Scientific Datasets, pages 843–856. Springer Berlin Heidelberg, 2012.
- [13] Navjot Kukreja, Jan Hüchelheim, Michael Lange, Mathias Louboutin, Andrea Walther, Simon W Funke, and Gerard Gorman. High-level python abstractions for optimal checkpointing in inversion problems. *arXiv preprint arXiv:1802.02474*, 2018.
- [14] Peter Lindstrom. Fixed-rate compressed floating-point arrays. *IEEE transactions on visualization and computer graphics*, 20(12):2674–2683, 2014.
- [15] M. Louboutin, M. Lange, F. Luporini, N. Kukreja, P. A. Witte, F. J. Herrmann, P. Velesko, and G. J. Gorman. Devito: an embedded domain-specific language for finite differences and geophysical exploration. *CoRR*, abs/1808.01995, Aug 2018.
- [16] F. Luporini, M. Lange, M. Louboutin, N. Kukreja, J. Hüchelheim, C. Yount, P. Witte, P. H. J. Kelly, G. J. Gorman, and F. J. Herrmann. Architecture and performance of Devito, a system for automated stencil computation. *CoRR*, abs/1807.03032, jul 2018.
- [17] Molly A. O’Neil and Martin Burtscher. Floating-point data compression at 75 gb/s on a GPU. In *Proceedings of the Fourth Workshop on General Purpose Processing on Graphics Processing Units*. ACM, 2011.
- [18] R-É Plessix. A review of the adjoint-state method for computing the gradient of a functional with geophysical applications. *Geophysical Journal International*, 167(2):495–503, 2006.
- [19] Michel Schanen, Oana Marin, Hong Zhang, and Mihai Anitescu. Asynchronous two-level checkpointing scheme for large-scale adjoints in the spectral-element solver nek5000. In *ICCS*, pages 1147–1158, 2016.
- [20] Athanassios Skodras, Charilaos Christopoulos, and Touradj Ebrahimi. The JPEG 2000 still image compression standard. *IEEE Signal processing magazine*, 18(5):36–58, 2001.
- [21] Philipp Stumm and Andrea Walther. Multistage approaches for optimal offline checkpointing. *SIAM Journal on Scientific Computing*, 31(3):1946–1967, 2009.
- [22] Jean Virieux, Stéphane Operto, Hafedh Ben-Hadj-Ali, Romain Brossier, Vincent Etienne, Florent Sourbier, Luc Giraud, and Azzam Haidar. Seismic wave modeling for seismic imaging. *The Leading Edge*, 28(5):538–544, 2009.
- [23] Qiqi Wang, Parviz Moin, and Gianluca Iaccarino. Minimal repetition dynamic checkpointing algorithm for unsteady adjoint calculation. *SIAM Journal on Scientific Computing*, 31(4):2549–2567, 2009.
- [24] Pengliang Yang, Jinghuai Gao, and Baoli Wang. RTM using effective boundary saving: A staggered grid GPU implementation. *Computers & Geosciences*, 68:64–72, 2014.
- [25] Yu Zhang, Houzhu Zhang, and Guanquan Zhang. A stable TTI reverse time migration and its implementation. *Geophysics*, 76(3):WA3–WA11, 2011.

The submitted manuscript has been created by UChicago Argonne, LLC, Operator of Argonne National Laboratory (‘Argonne’). Argonne, a U.S. Department of Energy Office of Science laboratory, is operated under Contract No. DE-AC02-06CH11357. The U.S. Government retains for itself, and others acting on its behalf, a paid-up nonexclusive, irrevocable worldwide license in said article to reproduce, prepare derivative works, distribute copies to the public, and perform publicly and display publicly, by or on behalf of the Government. The Department of Energy will provide public access to these results of federally sponsored research in accordance with the DOE Public Access Plan. <http://energy.gov/downloads/doe-public-access-plan>.